



# Predicting Dissolved Lignin Phenol Concentrations in the Coastal Ocean from Chromophoric Dissolved Organic Matter (CDOM) Absorption Coefficients

Cédric G. Fichot<sup>1\*†</sup>, Ronald Benner<sup>1,2</sup>, Karl Kaiser<sup>1,3</sup>, Yuan Shen<sup>1</sup>, Rainer M. W. Amon<sup>3</sup>, Hiroshi Ogawa<sup>4</sup> and Chia-Jung Lu<sup>4</sup>

<sup>1</sup> Marine Science Program, University of South Carolina, Columbia, SC, USA, <sup>2</sup> Department of Biological Sciences, University of South Carolina, Columbia, SC, USA, <sup>3</sup> Departments of Marine Sciences and Oceanography, Texas A&M University, Galveston, TX, USA, <sup>4</sup> Atmosphere and Ocean Research Institute, The University of Tokyo, Kashiwa, Japan

## OPEN ACCESS

### Edited by:

Christopher Osburn,  
North Carolina State University, USA

### Reviewed by:

Paul James Mann,  
Northumbria University Newcastle, UK  
Rossana Del Vecchio,  
University of Maryland, USA

### \*Correspondence:

Cédric G. Fichot  
cgfichot@gmail.com

### †Present Address:

Cédric G. Fichot,  
Jet Propulsion Laboratory, California  
Institute of Technology, Pasadena, CA,  
USA

### Specialty section:

This article was submitted to  
Marine Biogeochemistry,  
a section of the journal  
Frontiers in Marine Science

**Received:** 01 October 2015

**Accepted:** 21 January 2016

**Published:** 18 February 2016

### Citation:

Fichot CG, Benner R, Kaiser K,  
Shen Y, Amon RMW, Ogawa H and  
Lu C-J (2016) Predicting Dissolved  
Lignin Phenol Concentrations in the  
Coastal Ocean from Chromophoric  
Dissolved Organic Matter (CDOM)  
Absorption Coefficients.  
Front. Mar. Sci. 3:7.  
doi: 10.3389/fmars.2016.00007

Dissolved lignin is a well-established biomarker of terrigenous dissolved organic matter (DOM) in the ocean, and a chromophoric component of DOM. Although evidence suggests there is a strong linkage between lignin concentrations and chromophoric dissolved organic matter (CDOM) absorption coefficients in coastal waters, the characteristics of this linkage and the existence of a relationship that is applicable across coastal oceans remain unclear. Here, 421 paired measurements of dissolved lignin concentrations (sum of nine lignin phenols) and CDOM absorption coefficients [ $a_g(\lambda)$ ] were used to examine their relationship along the river-ocean continuum (0–37 salinity) and across contrasting coastal oceans (sub-tropical, temperate, high-latitude). Overall, lignin concentrations spanned four orders of magnitude and revealed a strong, non-linear relationship with  $a_g(\lambda)$ . The characteristics of the relationship (shape, wavelength dependency, lignin-composition dependency) and evidence from degradation indicators were all consistent with lignin being an important driver of CDOM variability in coastal oceans, and suggested physical mixing and long-term photodegradation were important in shaping the relationship. These observations were used to develop two simple empirical models for estimating lignin concentrations from  $a_g(\lambda)$  with a  $\pm 20\%$  error relative to measured values. The models are expected to be applicable in most coastal oceans influenced by terrigenous inputs.

**Keywords:** chromophoric dissolved organic matter, lignin, lignin-derived phenols, chromophore, absorption coefficient, coastal ocean, degradation indicators, photodegradation

## INTRODUCTION

Lignin is a major biochemical component of vascular plant tissues, and a well-established biomarker of terrigenous organic matter in the ocean. Lignin is a complex aromatic heteropolymer that binds cellulose and hemicellulose microfibrils in the secondary cell wall of xylem tissues, and provides biomechanical support to stems in vascular plants. Lignin is exclusively produced on land by vascular plants, with the exception of an intertidal red seaweed *Calliarthron cheilosporioides*

(Martone et al., 2009). During decomposition of plant matter by microorganisms in litter and soils, some lignin is mobilized in particulate or dissolved form to nearby streams and rivers (Aiken et al., 1985; Aiken and Cotsaris, 1995; Eriksson, 2010). Lignin eventually reaches the ocean, where its vascular-plant origin makes it an unambiguous biomarker of terrigenous organic matter (Hedges et al., 1997). As a result, lignin extracted from seawater and marine sediments has long been used to derive qualitative and quantitative information about the origins, transformations, and fates of terrigenous organic matter in the ocean (Opsahl and Benner, 1997; Hernes and Benner, 2006; Goni et al., 2008; Amon et al., 2012; Fichot and Benner, 2014; Tesi et al., 2014; Medeiros et al., 2015).

Dissolved lignin molecules are also chromophores, and evidence suggests they contribute significantly to the optical properties of chromophoric dissolved organic matter (CDOM) in natural waters. Lignin is an aromatic macromolecule, and is therefore an efficient absorber of ultraviolet radiation in natural waters (Chin et al., 1994; Weishaar and Aiken, 2001; Schmidt, 2010). The complex macromolecular structure of lignin is also thought to promote a continuum of intramolecular charge-transfer interactions that extend the absorption properties of lignin well into the visible region of the solar spectrum (Furman and Lonsky, 1988a,b; Del Vecchio and Blough, 2004; Boyle et al., 2009). As a result, strong linear relationships between dissolved lignin concentrations and absorption and fluorescence properties of CDOM have been observed in various estuarine and coastal environments (Hernes and Benner, 2003; Spencer et al., 2008; Hernes et al., 2009; Walker et al., 2009; Osburn and Stedmon, 2011; Fichot and Benner, 2012; Fichot et al., 2013; Yamashita et al., 2015). The ubiquity of correlations between CDOM and dissolved lignin in river-influenced ocean margins suggests lignin could be an important driver of the variability of CDOM optical properties in such systems. This strong linkage also suggests CDOM optical properties could serve as practical optical proxies for the concentration of this terrigenous biomarker in the ocean.

The utility of CDOM as a proxy for lignin concentration hinges strongly on the existence of relationships that are applicable to most river-influenced environments, and on an understanding of the factors driving and impacting these relationships. Despite the various reports of linkages between CDOM and dissolved lignin, the general characteristics of the CDOM-lignin relationship and of its drivers along the river-ocean continuums of the coastal ocean remains poorly known. Differences in the origin and alteration of CDOM and lignin, or the occurrence of non-lignin and non-covarying components of CDOM are examples of factors that can impact the lignin-CDOM relationship and jeopardize the utility of the proxy. Here, we investigated the relationship between dissolved lignin and CDOM absorption coefficients in the ultraviolet range (250–400 nm) using a large and fairly comprehensive data set ( $n = 421$ ) that spanned the full salinity gradient and multiple types of coastal systems in the global ocean. The objectives of this study were to reveal the characteristics of the relationship between CDOM absorption and dissolved lignin concentration in the ocean, provide insights about the factors driving and affecting the relationship, and provide simple models for predicting dissolved

lignin concentration from CDOM absorption coefficients that are widely applicable in terrestrially-influenced coastal systems.

## MATERIALS AND METHODS

### Field Sampling Overview and Study Regions

Field samples were collected from a wide variety of rivers, estuaries, and coastal waters across the northern hemisphere (Figure 1 and Table 1). A total of 421 paired water samples for CDOM and dissolved lignin analyses were collected as part of different research projects between September 2005 and October 2013. Nine different coastal-ocean areas off North America and Asia were sampled and encompassed subtropical, temperate, and arctic environments. A majority of samples was collected in waters from or influenced by rivers that contrast in terms of discharge dynamics and drainage-basin vegetation (e.g., Mississippi, Atchafalaya, Delaware, Susquehanna, Hudson, Connecticut, Mackenzie, Ob, Yukon, Noatak, Lena, and Yenisey). Two study regions stood out: (1) the Chukchi Sea was an area of high biological productivity that received less riverine inputs compared to the other regions (Cota et al., 1996; Grebmeier, 2012; Shen et al., 2012a; Palmer et al., 2013), and (2) the Otsuchi Bay was influenced by rivers with small drainage basins, steep slopes, and short residence times (Fukuda et al., 2007). Some samples in this data set (e.g., northern Gulf of Mexico, South Carolina Coast, Middle Atlantic Bight) were also collected in waters influenced by coastal wetlands and marshes. Finally, a significant number of samples were also representative

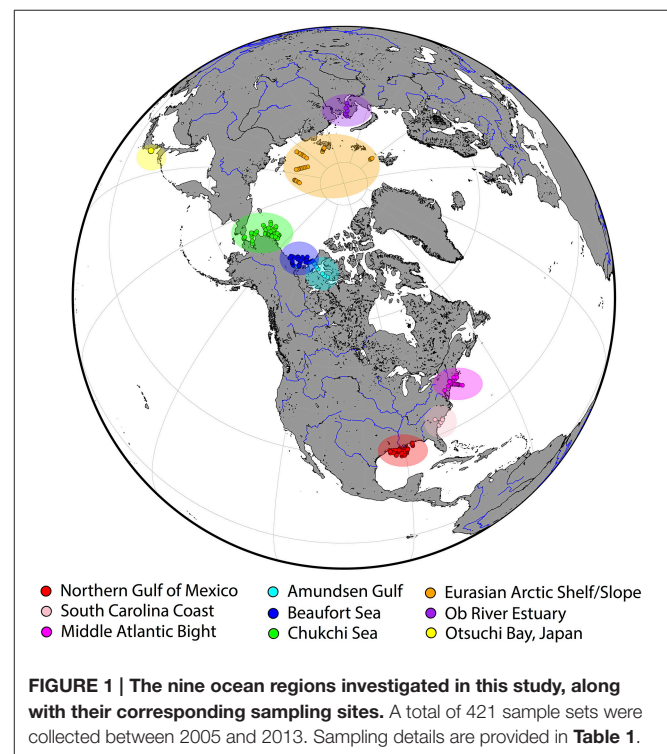


**TABLE 1 | General sampling information.**

	Research project*	Sampling period	Number of samples	Salinity range	Sample depth range	Related publications†
Gulf of Ob	–	September 2005	9	0–17.61	Surface	Fichot et al., 2013
Amundsen Gulf	CFL	July–August 2008	38	4.40–34.85	Surface–500 m	Fichot et al., 2013
Eurasian Arctic Shelf and Slope	NABOS	November 2008	54	27.53–34.97	Surface–700 m	Fichot et al., 2013
Northern Gulf of Mexico	GulfCarbon	January 2009	17	0–36.39	Surface	Fichot and Benner, 2011
		April 2009	22	0–36.95	Surface	Shen et al., 2012b
		July 2009	21	0–36.59	Surface	Fichot and Benner, 2012
		October–November 2009	22	0–36.55	Surface	Fichot et al., 2013
		March 2010	20	0–32.16	Surface	Fichot et al., 2014
Beaufort Sea	Malina	September 2009	80	0–34.87	Surface–1000 m	Fichot and Benner, 2014 Fichot et al., 2013
Chukchi Sea	ICESCAPE	June–July 2010	74	29.07–33.99	Surface–200 m	Fichot et al., 2013
South Carolina coast	–	Aug–November 2011	6	0–35.10	Surface	Fichot and Benner, 2014
Otsuchi Bay, Japan	TEAMS	September 2012	6	31.96–32.72	Surface	–
		November 2012	7	0–33.67	Surface	–
US Mid-Atlantic Bight	UNOLS Chief Scientist Training Cruise	October 2013	45	0–35.95	Surface–2800 m	–
Total			421	0–36.95	Surface–2800 m	

The corresponding sampling areas and sites are shown in **Figure 1**. A total of 160 measurements were acquired below the surface (i.e., sample depth >20 m).

\*CFL, Circumpolar Flaw Lead; NABOS, Nansen and Amundsen Basin Observational System; ICESCAPE, Impacts of Climate on the Eco-Systems and Chemistry of the Arctic Pacific Environment; TEAMS, Tohoku Ecosystem-Associated Marine Science; UNOLS, University-National Oceanographic Laboratory System.

†Peer-reviewed publication(s) in which part or all of the research project's data [TDLP<sub>9</sub> and  $a_g(\lambda)$ ] has previously been used.

of oligotrophic, subsurface (e.g., Arctic halocline), and deep-water environments (e.g., North Atlantic Deep Water). Overall, samples were collected during different seasons from waters spanning salinities ranging from 0 to 37, depths ranging from 0 to 2800 m, and water types ranging from nutrient-rich riverine waters to oligotrophic marine waters.

## CDOM Sampling and Analysis

Most samples for CDOM analysis were gravity filtered from Niskin bottles using Whatman Polycap Aqueous Solution (AS) cartridges (0.2- $\mu$ m pore size), collected in pre-combusted borosilicate glass vials, and stored immediately at 4°C until analysis in the laboratory. A few samples were collected using a bucket and filtered using a peristaltic pump through the Whatman Polycap Aqueous Solution (AS) cartridges. Absorbance of the samples was measured from  $\lambda = 250$ –800 nm using an ultraviolet (UV)-visible dual-beam spectrophotometer (Shimadzu UV-1601 or UV-2401PC/2501PC) and 10-cm quartz cells. For riverine and low-salinity samples (salinity < 10), 5-cm quartz cells or 1-cm quartz cuvettes were used. An exponential fit of the absorbance spectrum over an optimal spectral range was used to derive an offset value that was subtracted from the absorbance spectrum (Fichot and Benner, 2011). The optimal spectral range for the fit was typically 400–700 nm, but was adjusted for each sample (e.g., 350–700, 450–700 nm) as to provide the best fit of the absorbance spectrum possible over that spectral range. Absorbance corrected for offset was then

converted to Napierian absorption coefficients,  $a_g(\lambda)$  ( $\text{m}^{-1}$ ). The dependence of  $a_g(\lambda)$  on  $\lambda$  is described using Equation (1):

$$a_g(\lambda) = a_g(\lambda_0) \cdot \exp(-S(\lambda - \lambda_0)) \quad (1)$$

where  $\lambda_0 < \lambda$  and  $S$  is the spectral slope coefficient in the  $\lambda_0$ – $\lambda$  nm spectral range. A careful examination of each  $a_g(\lambda)$  spectrum demonstrated the  $a_g(\lambda)$ -values (especially for  $\lambda > 350$  nm) were well above the uncertainty of the measurement ( $\pm 0.005 \text{ m}^{-1}$  at  $\lambda = 400$  nm, for a 10-cm pathlength). The spectral slope coefficient of CDOM between 275 and 295 nm,  $S_{275-295}$ , was calculated as the slope of the linear regression of  $\ln[a_g(\lambda)]$  on  $\lambda$ , between  $\lambda = 275$  and 295 nm (Helms et al., 2008; Fichot and Benner, 2011). The  $S_{275-295}$ -values are reported in  $\text{nm}^{-1}$ .

## Lignin Sampling and Analysis

Samples for lignin analysis (1–10 L) were gravity filtered from Niskin bottles using Whatman Polycap AS cartridges (0.2- $\mu$ m pore size), acidified to pH = 2.5–3 with sulfuric acid, and extracted within a few hours using C-18 cartridges (Louchouart et al., 2000). Cartridges were stored at 4°C until elution with 30 mL of methanol (HPLC-grade). The eluent was stored in sealed, pre-combusted glass vials at –20°C until analysis. Lignin phenols were analyzed using the CuO oxidation method of Kaiser and Benner (2012). Concentrations of lignin phenols were measured as trimethylsilyl derivatives using an Agilent 7890 gas chromatograph equipped with a Varian DB5-MS capillary column and an Agilent 5975 mass selective

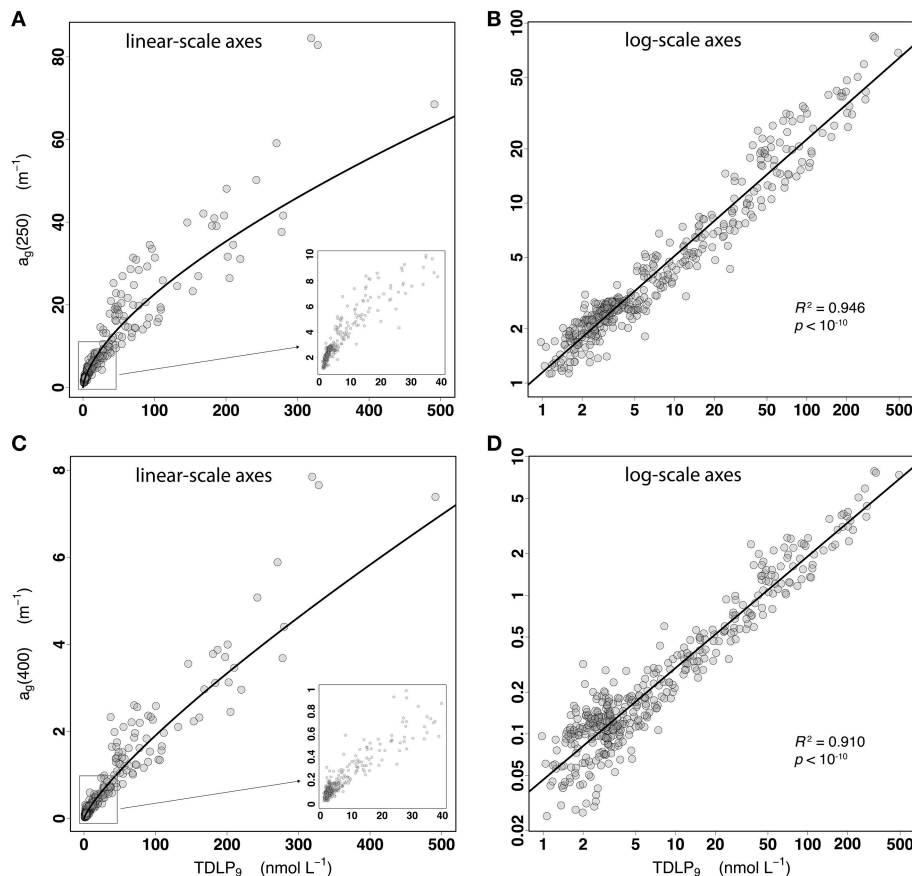


**FIGURE 2 | (A,B)** Scatter plots of  $a_g(250)$  vs.  $\text{TDLP}_9$  for the entire data set ( $n = 421$ ) displayed using linear-scale and log-scale axes, respectively. The inset in **(A)** is a close-up of the relationship for the lower  $a_g(250)$  and  $\text{TDLP}_9$ -values. The coefficient of determination ( $R^2$ ) and  $p$ -value of the linear regression of  $\ln[a_g(250)]$  on  $\ln(\text{TDLP}_9)$  are shown in **(B)**. **(C,D)** Same as **(A,B)** but for  $a_g(400)$ .

detector. The sum of nine lignin phenols was calculated as the total lignin phenol concentration: *p*-hydroxybenzaldehyde (PAL), *p*-hydroxyacetophenone (PON), *p*-hydroxybenzoic acid (PAD), vanillin (VAL), acetovanillone (VON), vanillic acid (VAD), syringaldehyde (SAL), acetosyringone (SON), and syringic acid (SAD). The sum of nine *p*-hydroxy, vanillyl, and syringyl lignin phenols is denoted as  $\text{TDLP}_9$  and is reported in units of  $\text{nmol L}^{-1}$ . The sums of concentrations of the three *p*-hydroxy phenols (PAL+PON+PAD), three vanillyl phenols (VAL+VON+VAD), and three syringyl phenols (SAL+SON+SAD) were also calculated, and are denoted here as P, V, and S phenols. All values of P, V, and S phenols are reported in units of  $\text{nmol L}^{-1}$ . The P/V and S/V ratios were also calculated and are unitless.

## Models

The models presented in this work for predicting dissolved lignin concentration from CDOM absorption coefficients were developed using the R environment for statistical computing and graphics and the “lm {stats}” function, obtained from the Comprehensive R Archive Network (<https://cran.r-project.org>).

## RESULTS AND DISCUSSION

### The Relationship between Lignin and CDOM Absorption Coefficients Across Coastal Oceans

A strong, non-linear relationship between dissolved lignin concentrations and the ultraviolet (UV) absorption coefficients of CDOM was observed over the full range of lignin concentrations measured in this study (**Figures 2A,C**). Dissolved lignin concentrations,  $\text{TDLP}_9$ , ranged more than 500-fold from  $<1$  to  $491 \text{ nmol L}^{-1}$ , and the CDOM absorption coefficient,  $a_g(\lambda)$ , ranged 85-fold at  $\lambda = 250 \text{ nm}$  ( $1.1\text{--}84.5 \text{ m}^{-1}$ ), and 300-fold at  $\lambda = 400 \text{ nm}$  ( $0.025\text{--}7.8 \text{ m}^{-1}$ ). The relationship between  $\text{TDLP}_9$  and  $a_g(\lambda)$  followed a relatively well-behaved exponential over the wide range of lignin concentrations and coastal environments sampled, thereby indicating that the observed variations in CDOM UV absorption are tightly linked to changes in lignin along the river-ocean continuum (**Figures 2A,C**). The concave-down shape of the exponential (**Figures 2A,C**) further indicated that the rate of decrease of  $a_g(\lambda)$  relative to that of  $\text{TDLP}_9$  (i.e., the derivative of the fitted line) increased substantially as lignin

concentration decreased along the river-ocean continuum. At 250 nm, this rate increased about nine-fold from 0.09 to 0.75 L nmol<sup>-1</sup> m<sup>-1</sup>, meaning  $a_g(250)$  decreased 9 times faster in high-salinity waters than in low-salinity waters for the same 1 nmol L<sup>-1</sup> decrease in TDLP<sub>9</sub> along the river-ocean continuum. The exponential behavior was less accentuated at 400 nm, for which the rate increased only 3-fold from ~0.01 to 0.035 L nmol<sup>-1</sup> m<sup>-1</sup>.

Linear regressions of the form shown in Equation (2) provided adequate fits for the exponential relationship between TDLP<sub>9</sub> and  $a_g(\lambda)$  at any wavelength in the 250–400 nm range (Figures 2B,D, 3A).

$$\ln(a_g(\lambda)) = \alpha \cdot \ln(\text{TDLP}_9) + \beta \quad (2)$$

The relationship was stronger with  $a_g(250)$  than with  $a_g(400)$ , as indicated by the coefficient of determination ( $R^2$ ) of Equation (2) decreasing from 0.946 at 250 nm to 0.910 at 400 nm (Figures 2B,D). A comparison of the  $R^2$  for every wavelength between 250 and 400 nm further indicated the overall relationship was strongest ( $R^2 > 0.95$ ) at ~285 nm (Figure 3A). Despite the goodness of the regression, significant scatter around the fitted lines was evident. A close examination of the relationship between TDLP<sub>9</sub> and  $a_g(250)$  using log-scale axes (Figure 2B) revealed that the scatter was relatively uniform (i.e., homoscedastic) over the entire range of lignin concentration. In contrast, the scatter around the fit was much less uniform (i.e., heteroscedastic) for  $a_g(400)$ , and increased substantially and progressively with decreasing lignin concentration (Figure 2D). The linear relationship between TDLP<sub>9</sub> and  $a_g(400)$  was marginal ( $R^2 < 0.4$ ) when lignin concentration was <6 nmol L<sup>-1</sup>.

The strength of the relationship between dissolved lignin concentration and CDOM absorption was maximal in the UV-C region at low lignin concentrations, and shifted to the UV-A region at higher lignin concentrations (Figure 3B). Additional insights about the relationship were gained by comparing the  $R^2$  of Equation (2) for two subsets of the entire data set: 1) a “low-CDOM” subset ( $n = 263$ ) where  $a_g(250) < 4 \text{ m}^{-1}$ , and 2) a “high-CDOM” subset ( $n = 158$ ) where  $a_g(250) \geq 4 \text{ m}^{-1}$ . The  $R^2$  analysis using the “low-CDOM” subset (Figure 3B) revealed the relationship was optimal ( $R^2 \sim 0.7$ ) at 250–275 nm (UV-C region), but weakened progressively and rapidly with wavelength to reach a minimal value ( $R^2 \sim 0.35$ ) at 400 nm. The  $a_g(263)$  was the optimal predictor of TDLP<sub>9</sub> for the “low-CDOM” subset. However, the  $a_g(\lambda)$  in the UV-A region ( $\lambda > 320 \text{ nm}$ ) was generally a poor predictor of lignin concentration in waters less influenced by terrigenous inputs. Interestingly, the reverse trend was observed when examining the “high-CDOM” subset. The  $R^2$  analysis using the “high-CDOM” subset (Figure 3B) indicated the relationship was good at all wavelengths, but improved significantly from a minimum  $R^2 = 0.87$  at 250 nm to a  $R^2 \sim 0.92$  in the UV-A region (320–400 nm). As will be explained later, this shift from UV-A to UV-C is likely related to the progressive change in the molecular structure of lignin, and potentially, of other terrigenous chromophores co-varying with lignin. This shift also indicates that  $a_g(\lambda)$  at a single wavelength is not an optimal predictor for lignin concentration over the range of lignin concentration found in coastal oceans.

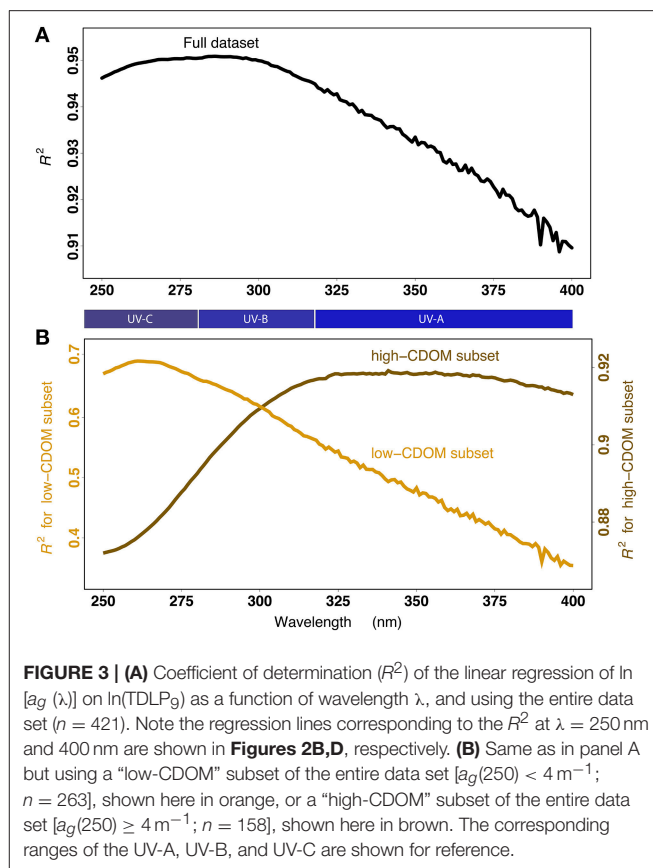
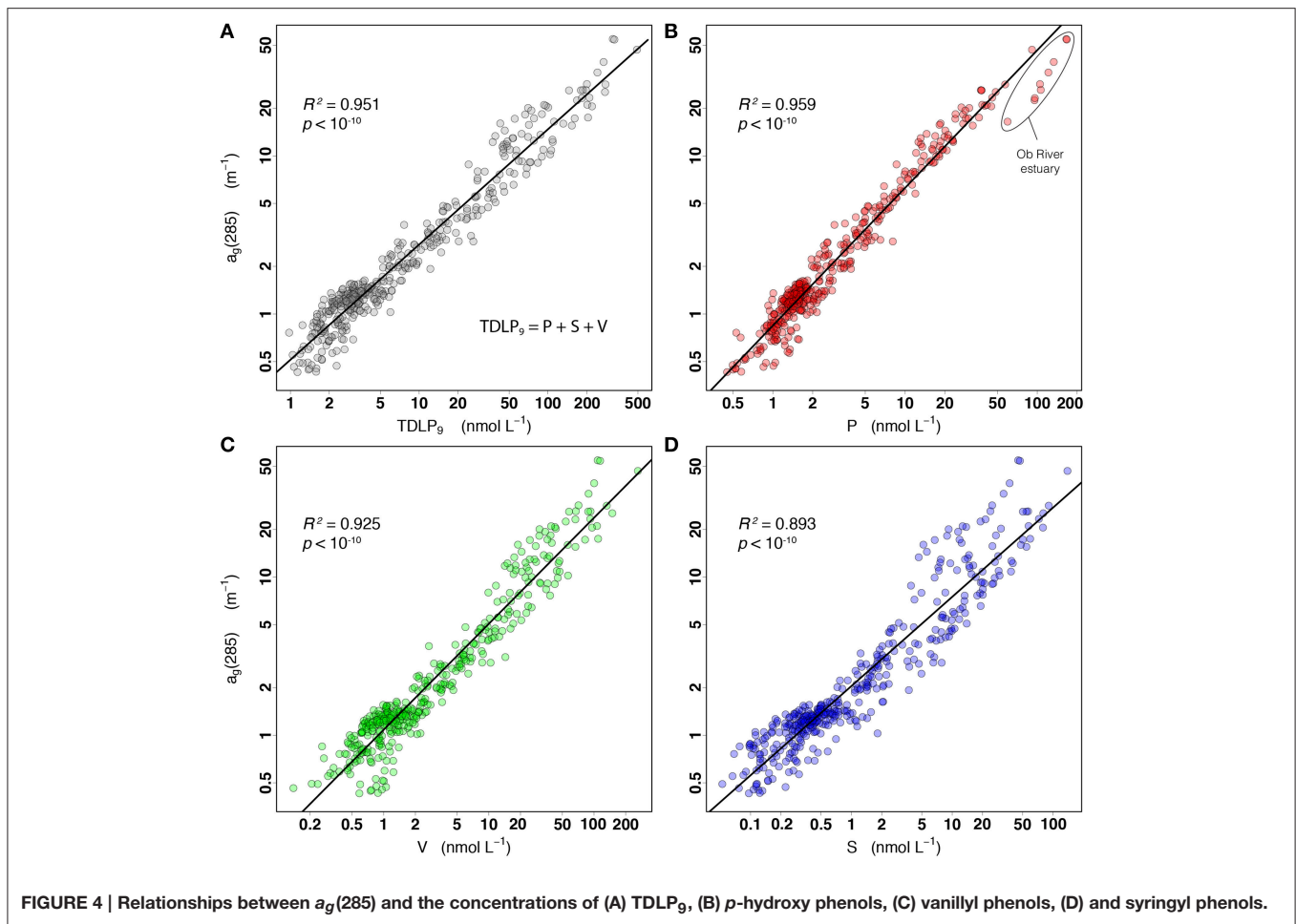


**FIGURE 3 | (A)** Coefficient of determination ( $R^2$ ) of the linear regression of  $\ln[a_g(\lambda)]$  on  $\ln(\text{TDLP}_9)$  as a function of wavelength  $\lambda$ , and using the entire data set ( $n = 421$ ). Note the regression lines corresponding to the  $R^2$  at  $\lambda = 250 \text{ nm}$  and  $400 \text{ nm}$  are shown in Figures 2B,D, respectively. **(B)** Same as in panel A but using a “low-CDOM” subset of the entire data set [ $a_g(250) < 4 \text{ m}^{-1}$ ;  $n = 263$ ], shown here in orange, or a “high-CDOM” subset of the entire data set [ $a_g(250) \geq 4 \text{ m}^{-1}$ ;  $n = 158$ ], shown here in brown. The corresponding ranges of the UV-A, UV-B, and UV-C are shown for reference.

The *p*-hydroxy phenols (P), vanillyl phenols (V), and syringyl phenols (S) that make up TDLP<sub>9</sub> exhibited varying degrees of correlation with the CDOM absorption coefficient (Figure 4). As explained earlier, the relationship between  $a_g(\lambda)$  and TDLP<sub>9</sub> was optimal at ~285 nm for the entire range of lignin concentrations ( $R^2 = 0.951$ ). The separation of TDLP<sub>9</sub> into P, V, and S phenols indicated the relationship between  $a_g(285)$  and P phenols across the full range of values was even stronger ( $R^2 = 0.959$ ) than with TDLP<sub>9</sub>. Only samples from the Ob estuary deviated significantly from the general relationship, and were enriched in P phenols relative to  $a_g(285)$ . However, this enrichment in P phenols was apparent and most likely originated from elevated levels of peat-derived sphagnum acid typically found in the Ob watershed, and their subsequent conversion into P phenols during the oxidation of lignin (Amon et al., 2012; Philben et al., 2014). The relationship became progressively less robust with V phenols ( $R^2 > 0.925$ ) and S phenols ( $R^2 > 0.893$ ). The trend is consistent with P phenols being more resistant to degradation in natural waters than V phenols, and with S phenols being the most susceptible to degradation (Opsahl and Benner, 1995; Benner and Opsahl, 2001; Benner and Kaiser, 2011). Furthermore, lignin produced by gymnosperms is devoid of S phenols, whereas P and V phenols are ubiquitous in lignin (Hedges and Mann, 1979; Benner and Opsahl, 2001; Shen et al., 2012b). This most likely impacted the relationship between  $a_g(285)$  and S phenols by making it sensitive to variations in watershed vegetation.



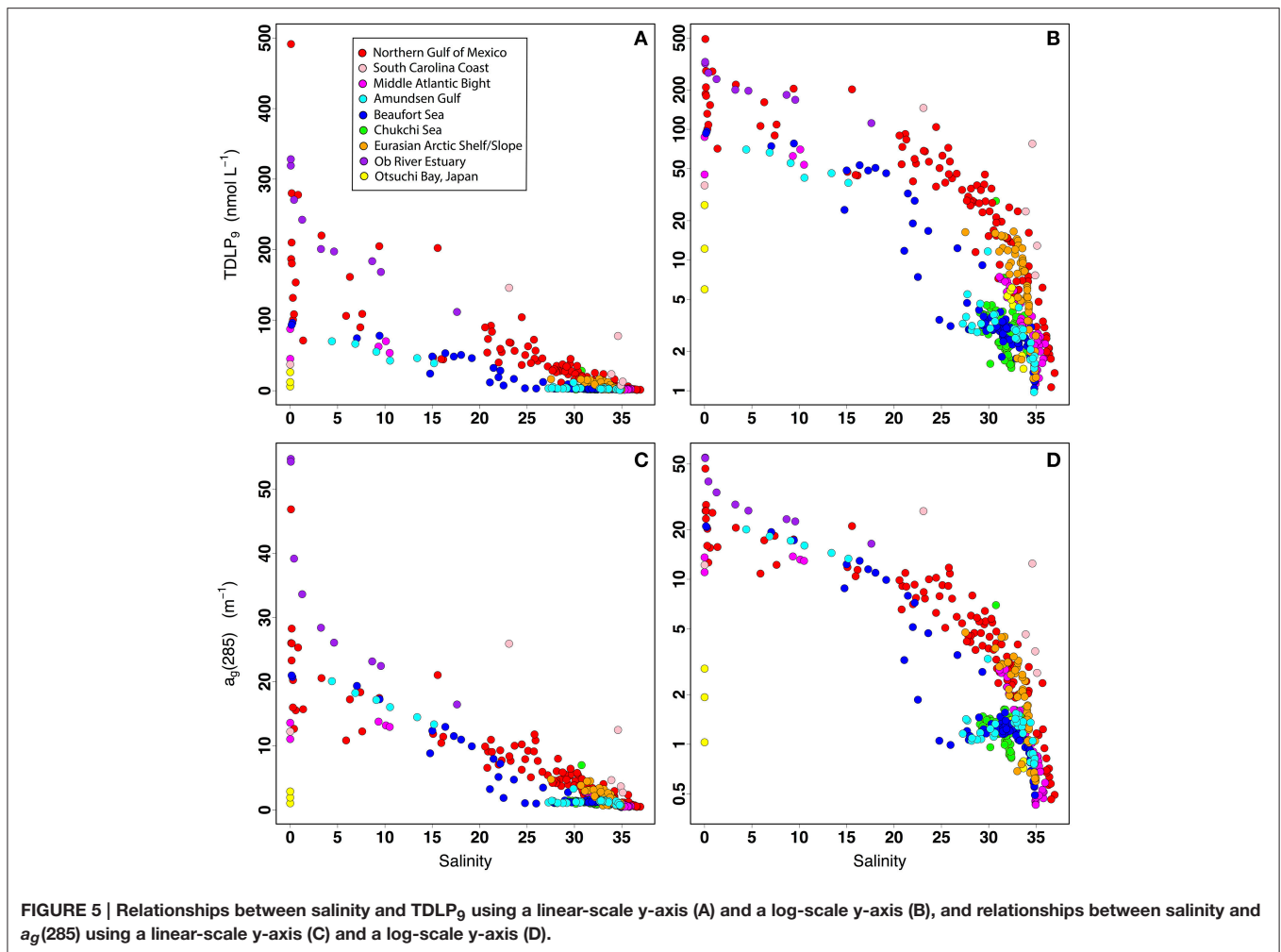
## Physical Mixing and Degradation Of Terrigenous CDOM

The decreasing trends in TDLP<sub>9</sub> concentrations and  $a_g(285)$  along the salinity gradient confirmed the importance of physical mixing in the distribution of these two variables along the river-ocean continuum (Figure 5). As expected from the strong relationship observed between TDLP<sub>9</sub> and  $a_g(285)$ , the relationships between salinity and TDLP<sub>9</sub> (Figures 5A,B) and between salinity and  $a_g(285)$  (Figures 5C,D) were strikingly similar. Although a large scatter in TDLP<sub>9</sub> and  $a_g(285)$  at salinities <5 and >35 indicated important differences among riverine sources and ocean end-members, the trends observed for each region clearly indicated physical mixing of riverine and oceanic end-members played a dominant role in regulating the variability of TDLP<sub>9</sub> and  $a_g(285)$  concentrations. Two South Carolina samples strongly influenced by salt-marsh inputs (Ashley River and Hunting Island, SC) stood out as being relatively enriched in CDOM and lignin, in agreement with previous observations that marsh-derived CDOM can be chemically and optically distinct (e.g., stronger absorption) from other estuarine CDOM (Tzortziou et al., 2008). In contrast, samples with salinities ~28–33 from the Western Arctic Ocean (Chukchi Sea, Beaufort Sea, Amundsen Gulf) stood out as being

relatively depleted in CDOM and lignin. Considering most of these samples were collected in regions experiencing extensive sea-ice melting, this relative depletion in CDOM and lignin was likely due to the presence of ice-melt water (low salinity and depleted in DOM).

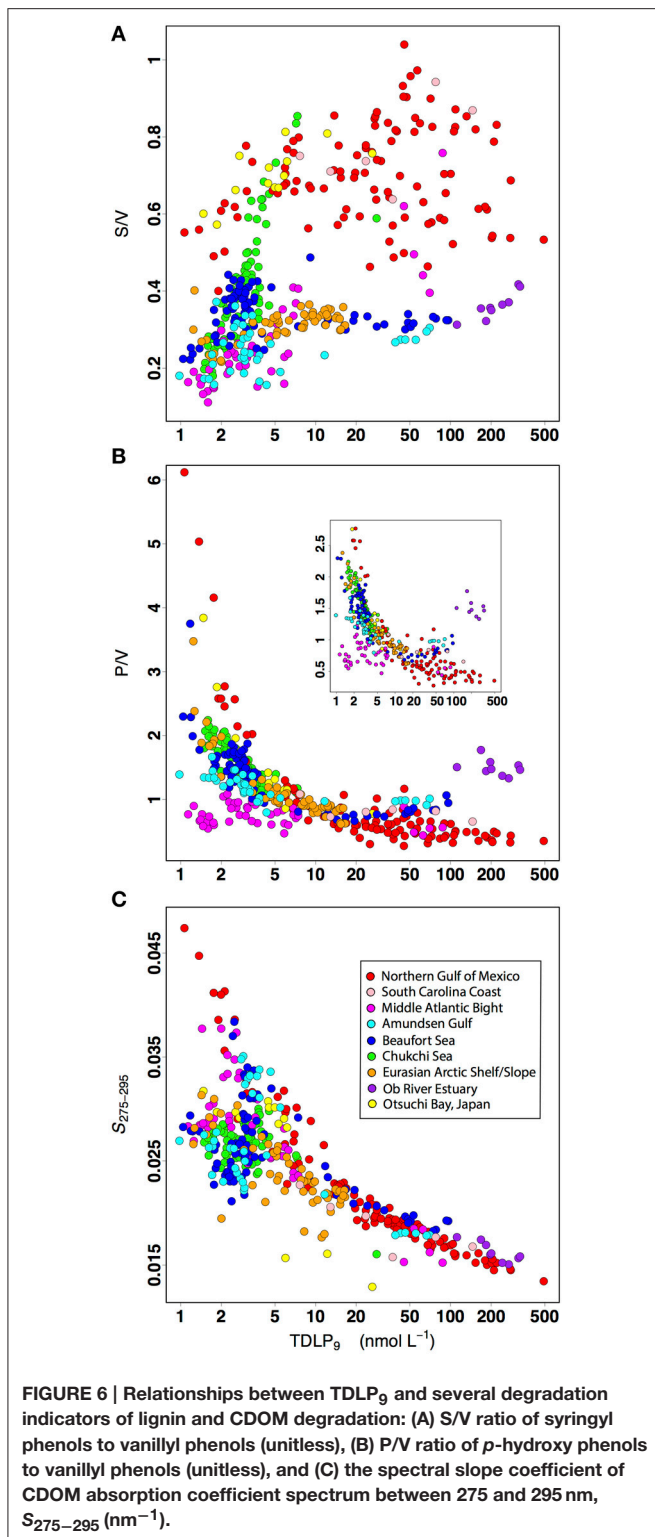
Several degradation indicators further indicated the general decrease in lignin concentrations from the rivers to the oligotrophic regions of coastal oceans was accompanied by a progressive change in the degradation state of terrigenous CDOM (Figure 6). The TDLP<sub>9</sub>-values decreased by almost four orders-of-magnitude along the river-ocean continuum. This decrease exhibited a weak, but significant and positive correlation ( $r = 0.51$ ) with the ratio of S to V phenols (S/V), and was accompanied by exponential increases in the ratio of P to V phenols (P/V) and the spectral slope coefficient of CDOM absorption ( $S_{275-295}$ ). These trends are consistent with similar observations along the salinity gradient of river-influenced ocean margins in previous studies, and with the physical mixing of two terrigenous CDOM end-members with different degradation states (Opsahl and Benner, 1998; Hernes and Benner, 2003; Helms et al., 2008; Fichot and Benner, 2012).

More specifically, the trends in S/V, P/V, and  $S_{275-295}$  observed herein are consistent with the physical mixing of two



end-members: (1) a relatively unaltered terrigenous CDOM end-member from rivers, and (2) a photochemically altered terrigenous CDOM end-member from the oligotrophic regions of the coastal oceans (Benner and Opsahl, 2001; Hernes and Benner, 2003; Fichot and Benner, 2012). The S/V has been shown to decrease during natural sunlight photodegradation experiments and during coupled photochemical-biological degradation experiments under simulated sunlight (Opsahl and Benner, 1998; Spencer et al., 2009; Benner and Kaiser, 2011). Note that Spencer et al. (2009) actually showed an increase in S/V after extreme exposure to solar radiation, but only after an initial decrease in S/V. The P/V has also been shown to increase during photodegradation experiments (Benner and Kaiser, 2011). In addition, the  $S_{275-295}$  has been shown to increase with decreasing molecular weight of CDOM and during exposure to solar radiation (Helms et al., 2008; Fichot and Benner, 2012; Yamashita et al., 2013). The trends in S/V, P/V, and  $S_{275-295}$  observed in this data set are consistent with the effects of photodegradation, and suggest the progressive change in the degradation state of terrigenous CDOM played an important role shaping the relationship between lignin and CDOM absorption coefficients.

The relatively weak correlation ( $r = 0.51$ ) between the S/V and TDLP<sub>9</sub> was not unexpected (Figure 6A). The S/V is not only affected by solar exposure, but is also a well-established indicator of the source vegetation of lignin and terrigenous DOM in natural waters (Hedges and Mann, 1979; Hedges and Ertel, 1982; Opsahl et al., 1999; Dittmar and Kattner, 2003; Shen et al., 2012b). As mentioned earlier, the S/V reflects the relative contributions of gymnosperm and angiosperm vegetation in lignin and terrigenous DOM because S phenols are not produced by gymnosperms. Lower S/V are thus typically measured in lignin that originates from gymnosperm-dominated watersheds (e.g., boreal forests), whereas higher S/V are indicative of significant contributions from angiosperms (e.g., tundra, deciduous forests). The effect of vegetation source on lignin phenol composition was evident in this data set, with low S/V values ( $< 0.5$ ) measured in Arctic waters. The drainage basins of large Arctic rivers are dominated by gymnosperms, and the S/V of Arctic rivers typically range from  $\sim 0.2$  to  $0.45$  (when calculated from nmol L<sup>-1</sup> concentrations) and exhibit some moderate variations with flow regime (Amon et al., 2012). The effect of vegetation was also evident from the high S/V values ( $> 0.5$ ) measured in the sub-tropical and temperate coastal oceans, which receive



substantial contributions from angiosperms. Some samples from the Chukchi Sea had relatively high S/V values, but these samples were strongly influenced by Pacific Ocean water or small rivers draining tundra. Finally, a large number of samples from the Middle Atlantic Bight had comparatively low S/V values. This

was likely observed because most of the terrigenous DOM on the shelf of the Middle Atlantic Bight shelf originates from gymnosperm-dominated environments further north, and is transported southward by currents (Chapman and Beardsley, 1989; Mountain, 1991).

Evidence suggests the P/V ratio is a useful indicator of the extent of lignin degradation. Here, the P/V increased several-fold and exponentially with decreasing lignin concentrations (**Figure 6B**). The P/V has been shown to increase substantially after continuous or intermittent solar exposure (Benner and Kaiser, 2011), and unlike the S/V, the P/V is not as sensitive to changes in source vegetation. The P phenols are widely distributed among vascular plants. However, as mentioned earlier, inputs from peatlands can increase the P/V, most likely as a result of the conversion of sphagnum acid into P phenols during CuO oxidation. Elevated concentrations of P phenols were observed in the peatland-influenced samples from the Ob River estuary, and to a much lesser degree, from the Mackenzie River estuary. Samples influenced by sub-tropical salt marshes (e.g., Terrebonne Bay, South Carolina Coast) also have slightly elevated values of P/V. Note the P/V can also reflect changes in the flow regime of rivers and be indicative of the <sup>14</sup>C age of terrigenous DOM immobilized (Amon et al., 2012). High P/V and lower lignin concentrations have thus been observed during base flow in Arctic Rivers, and the reverse observed during peak flow (Amon et al., 2012), suggesting that changes in river flow could contribute to the trends observed here between TDLP<sub>9</sub> and P/V. Finally, the highest P/V-values (>4) were observed in samples from oligotrophic eddies shed from the Loop Current and impinging on the continental shelf in the northern Gulf of Mexico (Schiller et al., 2011; Fichot et al., 2014). These high P/V were likely attributed to the long-term solar exposure and degradation in the optically clear Loop-Current waters, which originate in the Atlantic Ocean.

The exponential increase in S<sub>275–295</sub> with decreasing lignin concentrations was also consistent with physical mixing and the effects of photochemical degradation (**Figure 6C**). S<sub>275–295</sub> has been shown to increase during photodegradation and is a sensitive indicator of CDOM photodegradation in natural waters (Helms et al., 2008, 2013; Ortega-Retuerta et al., 2009; Fichot and Benner, 2012; Yamashita et al., 2013). Overall, the S<sub>275–295</sub> displayed a clear increasing trend with decreasing TDLP<sub>9</sub> concentrations in the present study. With the exception of a few outliers, S<sub>275–295</sub> increased monotonically with decreasing TDLP<sub>9</sub>-values ranging from 500 to 10 nmol L<sup>-1</sup>. When TDLP<sub>9</sub> was <10 nmol L<sup>-1</sup>, the relationship between S<sub>275–295</sub> and TDLP<sub>9</sub> split into two groups of data: one that continued to show a strong relationship between S<sub>275–295</sub> and TDLP<sub>9</sub>, and one that showed little correlation between the two. The first group consisted essentially of surface samples, whereas the second group corresponded primarily of sub-surface and deep waters, and of productive, high-latitude waters that were moderately influenced by terrigenous inputs (e.g., Chukchi Sea, Canada Basin, Amundsen Gulf). Limited solar exposure, a greater relative contribution of microbial degradation, or a more prominent influence of non-terrigenous sources of CDOM (*in situ* production) can be expected in these water types, and are



consistent with the relatively low  $S_{275-295}$ -values ( $\sim 0.025 \text{ nm}^{-1}$ ) observed. The limited solar exposure in sub-surface and deep water likely contributed to the lower  $S_{275-295}$ . Furthermore, previous studies reported  $S_{275-295}$ -values of  $\sim 0.025 \text{ nm}^{-1}$  for plankton-derived CDOM, and have provided evidence that  $S_{275-295}$  decreases slightly during microbial degradation (Ortega-Retuerta et al., 2009; Fichot and Benner, 2012).

It is important to understand that the progressive changes in the degradation state of terrigenous CDOM observed along the river-ocean continuum are largely driven by the physical mixing of riverine and ocean end-members (Fichot and Benner, 2012), and that the observed change largely reflects long-term effects of photochemical degradation on the ocean end-member of terrigenous CDOM. Terrigenous CDOM, which remains relatively unaltered in rivers, mixes with photochemically altered terrigenous CDOM from oligotrophic regions of ocean margins (Benner and Opsahl, 2001; Hernes and Benner, 2003; Fichot and Benner, 2012). Solar exposure in surface waters and the extent of photochemical degradation occurring over typical residence times of river water in ocean margins (e.g., months) has been shown to be relatively moderate, even in subtropical river-influenced ocean margins (Fichot and Benner, 2014). Much of the photochemical degradation occurs beyond the shelf where the residence time of the water is much longer and solar exposure in surface waters is strongly enhanced by a sharp increase in UV penetration relative to the mixed layer depth. In some cases, the terrigenous CDOM found in the oligotrophic regions of the coastal oceans can have a very different and more distant origin, as was the case in this data set when Loop-Current oligotrophic eddies impinged on the Northern Gulf of Mexico shelf (Fichot et al., 2014). In the Arctic Ocean, solar exposure and photodegradation are less than in subtropical regions, but the ocean end-member can have a more distant origin and the terrigenous CDOM can be more chemically altered (e.g., Pacific Water in Chukchi or Beaufort Seas, or Atlantic water off Svalbard).

The concave-down shape of the exponential relationship between  $\text{TDL}P_9$  and  $a_g(\lambda)$  was consistent with mixing and long-term photodegradation playing important roles in shaping the relationship between lignin concentration and CDOM absorption coefficients. Photodegradation has been shown to lead to a decrease in the molecular weight and aromaticity of terrigenous CDOM (Kieber et al., 1989, 1990; Opsahl and Benner, 1998; Miller et al., 2002; Helms et al., 2008). The molecular weight and aromaticity of a compound is, in turn, strongly linked to its molar absorptivity (Chin et al., 1994; Weishaar and Aiken, 2001), such that a given concentration of lignin in low-molecular-weight molecules absorbs much less efficiently than the same concentration of lignin within high-molecular weight molecules. The concave-down shape of the relationship indicated there was an acceleration in the loss of  $a_g(\lambda)$  relative to that of  $\text{TDL}P_9$  as lignin concentrations decreased from riverine to oligotrophic waters. A loss of absorption strictly due to the loss of chromophoric material (i.e., without a loss of molar absorptivity) would tend to produce a linear rather than a concave-down exponential relationship. Here, the acceleration in the loss of  $a_g(\lambda)$  was consistent with a progressive loss of molar

absorptivity superimposed on a loss of chromophoric material, and is consistent with previous observations of a decrease in molecular weight of both CDOM and lignin along the river-ocean continuum in ocean margins (Hernes and Benner, 2003; Helms et al., 2008).

The characteristics of the relationship between  $\text{TDL}P_9$  and  $a_g(400)$  were consistent with a progressive loss of intramolecular charge-transfer interactions in CDOM along the river-ocean continuum. Intramolecular charge-transfer interactions among chromophores in aromatic molecules such as lignin have been proposed as a mechanism to explain the exponential shape of the CDOM absorption spectrum and its absorption at wavelengths  $>350 \text{ nm}$  (Del Vecchio and Blough, 2004; Boyle et al., 2009; Sharpless and Blough, 2014). In this model, charge-transfer interactions among electron donors (e.g., phenols and/or methoxylated phenols in lignin) and electron acceptors (e.g., quinones or aromatic ketones/aldehydes in lignin) are thought to produce lower-energy optical transitions and enhance CDOM absorption at wavelengths  $>350 \text{ nm}$ . The contribution of electronic interactions to the CDOM absorption is linked to the molecular weight of terrigenous molecules like lignin, because compounds with higher molecular weight have a greater potential for intramolecular charge-transfer interactions. A sharp decrease in the molecular weight of lignin along the river-ocean continuum would therefore be associated with a loss of intramolecular charge-transfer interactions, and with a weakening contribution of lignin to the CDOM absorption at wavelengths  $>350 \text{ nm}$ . The worsening of the relationship between  $\text{TDL}P_9$  and  $a_g(400)$  with decreasing lignin concentrations, which eventually leads to an insignificant relationship between  $\text{TDL}P_9$  and  $a_g(400)$  in the more oligotrophic regions of the coastal oceans, is consistent with the effects of photodegradation.

## On the Contribution of Lignin and other Components to CDOM Absorption

The existence of a well-behaved relationship between  $\text{TDL}P_9$  and  $a_g(\lambda)$  from the rivers to the oligotrophic regions of several contrasting coastal oceans was a strong indication that lignin is generally an important driver of the variability of CDOM absorption coefficients in coastal waters. However, the contribution of lignin to the absorption coefficient of CDOM was not uniform across the 250–400 nm spectrum. Lignin appeared an important contributor to  $a_g(\lambda)$  in the UV-C ( $\lambda < 280 \text{ nm}$ ) and UV-B ( $280 < \lambda < 320 \text{ nm}$ ) regions over the entire range of lignin concentrations observed in this study. However, for  $\lambda > 350 \text{ nm}$ , lignin only seemed to contribute significantly to CDOM absorption for the upper range of  $\text{TDL}P_9$  concentrations and  $a_g(\lambda)$  values (e.g.,  $\text{TDL}P_9 > 10 \text{ nmol L}^{-1}$  or  $a_g(250) > 4 \text{ m}^{-1}$ ). For this upper range, lignin appeared an even greater contributor to  $a_g(\lambda)$  in the UV-A region than in the UV-B and UV-C regions. As described earlier, the spectral dependency of the relationship likely results from the change in the degradation state of terrigenous CDOM. The P phenols in lignin appeared to be the greater contributor to the absorption coefficients of CDOM, followed by the V phenols and the S phenols. A greater contribution of the P phenols to CDOM absorption is consistent

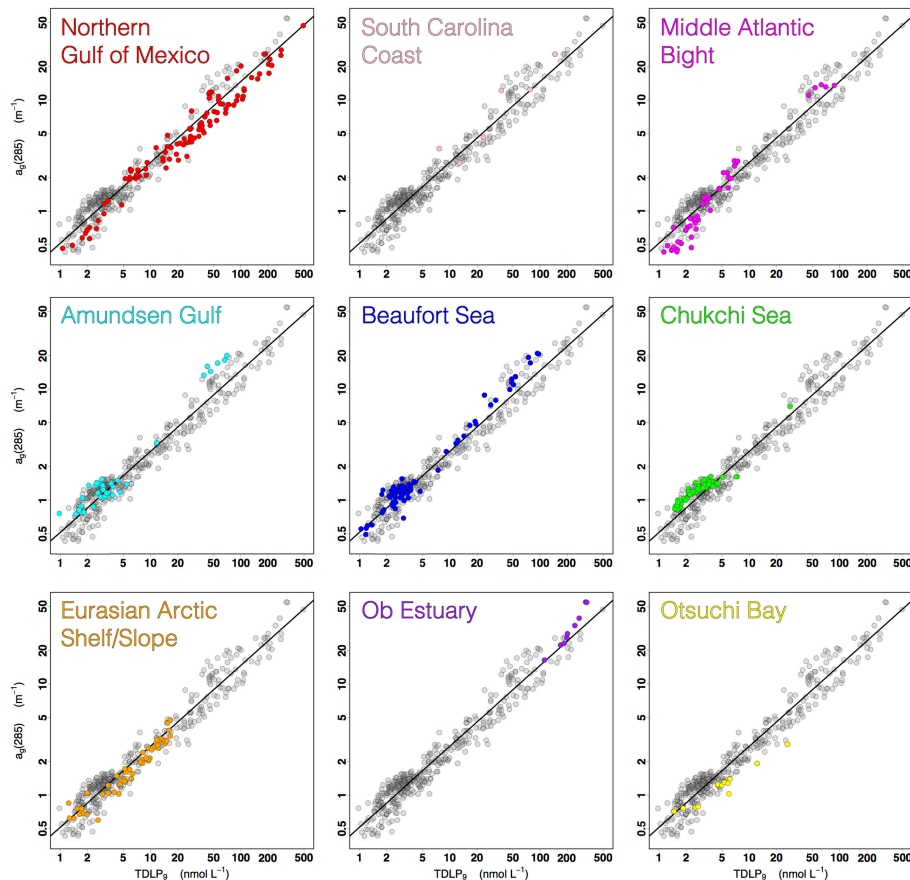


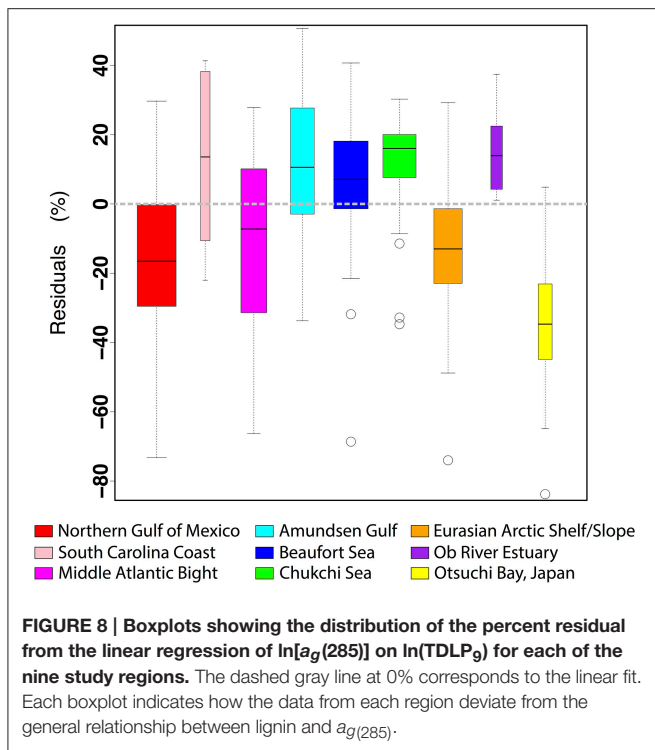
**FIGURE 7 |** Scatter plots of the relationship between  $a_g(285)$  and  $TDL P_9$  (log-scale axes) highlighting the data from each of the nine study regions.

with their greater resistance to photodegradation (Benner and Kaiser, 2011), and their selective preservation relative to the V and S phenols as lignin concentrations decrease along the river-ocean continuum. Although this is only speculation, it is possible the greater photochemical resistance of P phenols contributes to their preservation in higher molecular weight and more aromatic structures that have higher molar absorptivities and higher potential for intramolecular electronic interactions. The selective preservation of the P phenols is consistent with the strong relationship observed between P phenols and  $a_g(\lambda)$  in the more oligotrophic regions of the coastal oceans.

A variety of other chromophoric constituents in terrigenous DOM also likely contribute to CDOM absorption and impact the relationship between lignin and CDOM. Lignin has the chemical moieties necessary to make it an important chromophore (Boyle et al., 2009; Sharpless and Blough, 2014). It is important to recognize, however, that a variety of other chromophoric components in terrigenous DOM likely co-vary strongly with lignin, and can contribute significantly to the CDOM absorption despite the strong linkage observed between CDOM and lignin. Tannins, a class of polyphenols, are components of many terrestrial plant tissues (e.g., foliage, bark) and are readily released to aquatic systems (Benner et al., 1990; Hernes et al.,

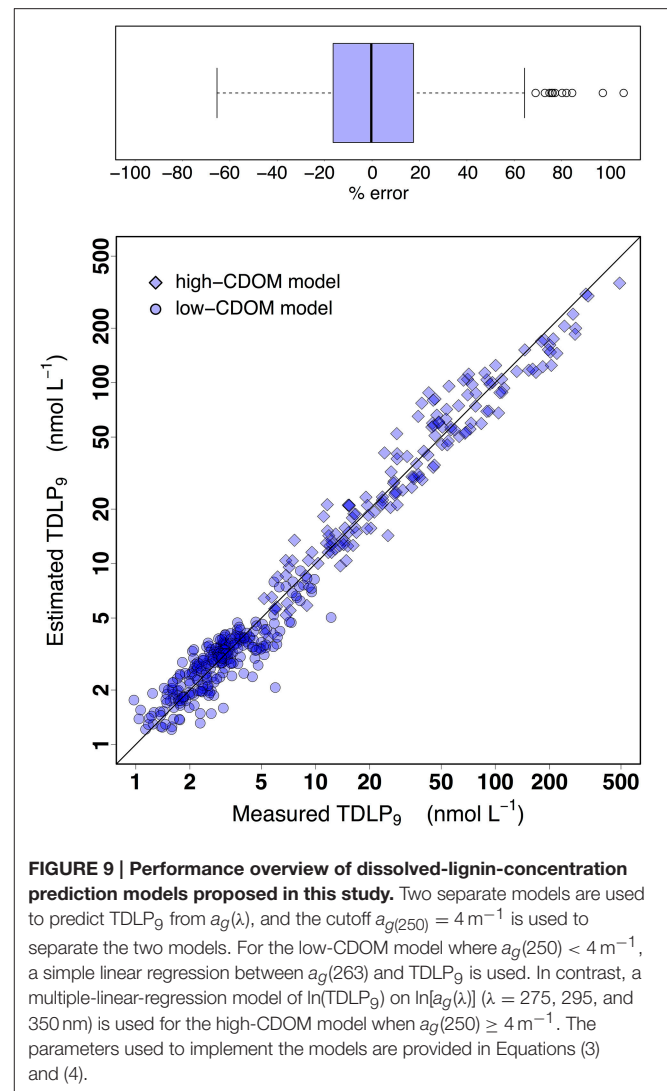
2001; Kraus et al., 2003; Maie et al., 2008). Dissolved tannins also absorb very strongly in the ultraviolet and visible region (Lawrence, 1980; Alberts, 1982; Kraus et al., 2003). However, previous studies have reported that tannin concentrations are very low in natural waters (Maie et al., 2006), and that microbial degradation, precipitation, sorption to sediments and potentially photodegradation removes tannins from aquatic systems (Benner et al., 1986; Hernes et al., 2001; Maie et al., 2008). The contribution of tannins to the CDOM absorption in coastal waters remains unclear, and more work is needed to directly assess the linkage between tannins and CDOM in coastal oceans.

Dissolved black carbon is a component of terrigenous DOM, and several studies indicate it is a potentially important component of DOC in natural waters (Kim et al., 2004; Mannino and Harvey, 2004; Ziolkowski and Druffel, 2010; Dittmar et al., 2012). Dissolved black carbon is thought to contribute up to 10% of the global riverine DOC flux to the ocean (Jaffé et al., 2013), and it contains condensed aromatic compounds that absorb strongly in the ultraviolet region (Russo et al., 2012). Stubbins et al. (2015) showed that dissolved black carbon concentration was more strongly correlated with  $a_g(250)$  than with  $a_g(400)$  for high-CDOM samples [ $a_g(250) \sim 10\text{--}150\text{ m}^{-1}$ ]. Interestingly, our study revealed the reverse trend for lignin, with



lignin concentration being more strongly correlated with  $a_g(400)$  than with  $a_g(250)$  for samples from a similar range of CDOM absorption [ $a_g(250) \sim 4\text{--}100\text{ m}^{-1}$ ]. These opposing trends are possibly linked to differences in the molecular structures of dissolved black carbon and dissolved lignin. Black carbon contains condensed aromatic compounds that typically have very high molar absorptivities in the UV (Chin et al., 1994; Weishaar and Aiken, 2001; Russo et al., 2012), whereas partially oxidized lignin contains the moieties responsible for intramolecular charge-transfer interactions, which are particularly effective at absorbing at wavelengths  $>350\text{ nm}$  (Del Vecchio and Blough, 2004; Boyle et al., 2009; Sharpless and Blough, 2014). Soils are a major source of black carbon and lignin, suggesting these two components likely correlate strongly in river-influenced coastal areas. More work is needed to better understand the potential contribution of black carbon to the optical properties of CDOM along the river-ocean continuum.

An analysis of the percent residuals from the linear fit of the  $a_g(285)$ – $\text{TDLP}_9$  relationship revealed some interesting variations among the different coastal oceans of this study (Figures 7, 8). Although deviations from the fitted line can occur for a variety of reasons, independent variations in the relative contributions of other, non-lignin components are likely a dominant factor. Plankton and microbes can also produce chromophoric compounds (e.g., amino acids, nucleic acids) that have variable effects on the CDOM dynamics of natural waters and will tend to contribute to the scatter in the relationship between  $\text{TDLP}_9$  and  $a_g(\lambda)$  (Rochelle-Newall and Fisher, 2002; Nelson et al., 2004; Yamashita and Tanoue, 2008; Ortega-Retuerta et al., 2009; Zhang et al., 2009; Fichot and Benner, 2012). Most of the samples from the Northern



Gulf of Mexico, Middle Atlantic Bight, Eurasian shelf, and Otsuchi Bay, exhibited elevated  $\text{TDLP}_9$ -values relative to  $a_g(285)$  (i.e., negative residuals), thereby suggesting lignin was a more dominant contributor to  $a_g(285)$  in these waters. The deviation was particularly strong in the Otsuchi Bay waters, which receives inputs from short and steep rivers with short water residence times. In contrast, most samples from the Amundsen Gulf, Beaufort Sea, Chukchi Sea, Ob estuary, and South Carolina coast exhibited relatively low  $\text{TDLP}_9$ -values compared to  $a_g(285)$  (i.e., positive residuals), suggesting a greater contribution of non-lignin chromophores. The positive residuals in the Chukchi Sea (all collected in summer) were potentially related to a higher background of autochthonous CDOM in these productive waters (Shen et al., 2012a), whereas those of the Ob estuary are consistent with significant contribution of non-lignin CDOM from *Sphagnum sp.* peats (Amon et al., 2012; Philben et al., 2014). The positive residuals in the South Carolina coast samples are likely related to contributions from the tidal marshes, which have been shown to have distinctive CDOM chemical and optical

properties (Tzortziou et al., 2008). Finally, many of the positive residuals were from samples collected in or near rivers during summer, and could be related to the *in situ* production of CDOM, or be related to depletion of lignin observed after the peak river flow during spring (Amon et al., 2012; Shen et al., 2012b).

## Empirical Models For Estimating TDLP<sub>9</sub> from $a_g(\lambda)$

Exploration of lignin and CDOM relationships provided useful information for the development of two simple empirical models for the retrieval of TDLP<sub>9</sub> from  $a_g(\lambda)$  in coastal oceans. The  $a_g(285)$  was, on average, the best single-wavelength predictor of TDLP<sub>9</sub> over the range of absorption coefficients and lignin concentrations observed in this study. However, the spectral dependency of the relationship indicated  $a_g(263)$  was the optimal single-wavelength predictor of TDLP<sub>9</sub> for samples where  $a_g(250) < 4 \text{ m}^{-1}$ , and  $a_g(350)$  was the optimal single-wavelength predictor for TDLP<sub>9</sub> for samples where  $a_g(250) \geq 4 \text{ m}^{-1}$ . Furthermore, photodegradation had a strong effect on the relationship, and  $S_{275-295}$  helped factor in this effect and improve the TDLP<sub>9</sub> predictions for high-CDOM samples, where  $S_{275-295}$  and TDLP<sub>9</sub> were most correlated [TDLP<sub>9</sub>  $\geq 10 \text{ nmol L}^{-1}$  or  $a_g(250) \geq 4 \text{ m}^{-1}$ ]. These observations guided the development of two sub-models separated by the  $a_g(250) = 4 \text{ m}^{-1}$  cutoff.

When  $a_g(250) < 4 \text{ m}^{-1}$ , a “low-CDOM” sub-model based on a simple linear regression was used,

$$\ln(\text{TDLP}_9) = 0.7672 \cdot a_g(263) - 0.3987 \quad (3)$$

When  $a_g(250) \geq 4 \text{ m}^{-1}$ , a “high-CDOM” sub-model based on a multiple linear regression was used,

$$\ln(\text{TDLP}_9) = -2.282 \cdot \ln(a_g(350)) - 8.209 \cdot \ln(a_g(275)) + 11.365 \cdot \ln(a_g(295)) + 2.909 \quad (4)$$

In the case of the multiple linear regression of Equation (4), all derived coefficients were significant by the *t*-test ( $p < 0.0005$ ), thereby confirming  $a_g(275)$  and  $a_g(295)$  represented meaningful additions to the model. The addition of  $a_g(275)$  and  $a_g(295)$  also improved the adjusted  $R^2$  of the regression (adj  $R^2 = 0.936$ ) relative to a single regression model using only  $a_g(350)$  (adj  $R^2 = 0.918$ ). The use of  $a_g(275)$  and  $a_g(295)$  in Equation (4) was somewhat similar to using  $S_{275-295}$  as one of the terms, but did not require the extra step of calculating  $S_{275-295}$ . Note the use of additional predictors in either Equation (3) or (4), or the use of partial-least-square regressions did not significantly improve the adjusted  $R^2$  of the regressions nor the % error of the estimates relative to these simple empirical models. This indicated the useful information contained in the spectral shape of CDOM was mostly exploited. Note here, that even though the predictor terms in Equation (4) are strongly correlated, multi-collinearity does not represent an issue for predictive models. Multi-collinearity is problematic when trying to interpret the meaning of the derived parameters in the equations.

Overall, these simple empirical models provide a practical means to derive reasonably accurate estimates of TDLP<sub>9</sub> from CDOM absorption coefficients in coastal oceans (Figures 9, 10). A comparison of the measured and estimated TDLP<sub>9</sub> indicated the model retrieved TDLP<sub>9</sub>-values that were on average within  $\pm 20\%$  of the measured values (Figure 9). The % error was  $< 17\%$  for half of all retrieved TDLP<sub>9</sub>-values, and it very rarely exceeded 60%. As it is currently parameterized, the model might slightly underestimate some of the very high lignin concentrations found in rivers ( $> 200 \text{ nmol L}^{-1}$ ). The capacity of the model to reproduce realistic distributions of TDLP<sub>9</sub> was also assessed for a cross-shelf section of the Middle Atlantic Bight (Figure 10). This subset of the data set was chosen because it encompassed a coastal region with a moderate gradient in TDLP<sub>9</sub>, and included data from both surface and sub-surface waters. The

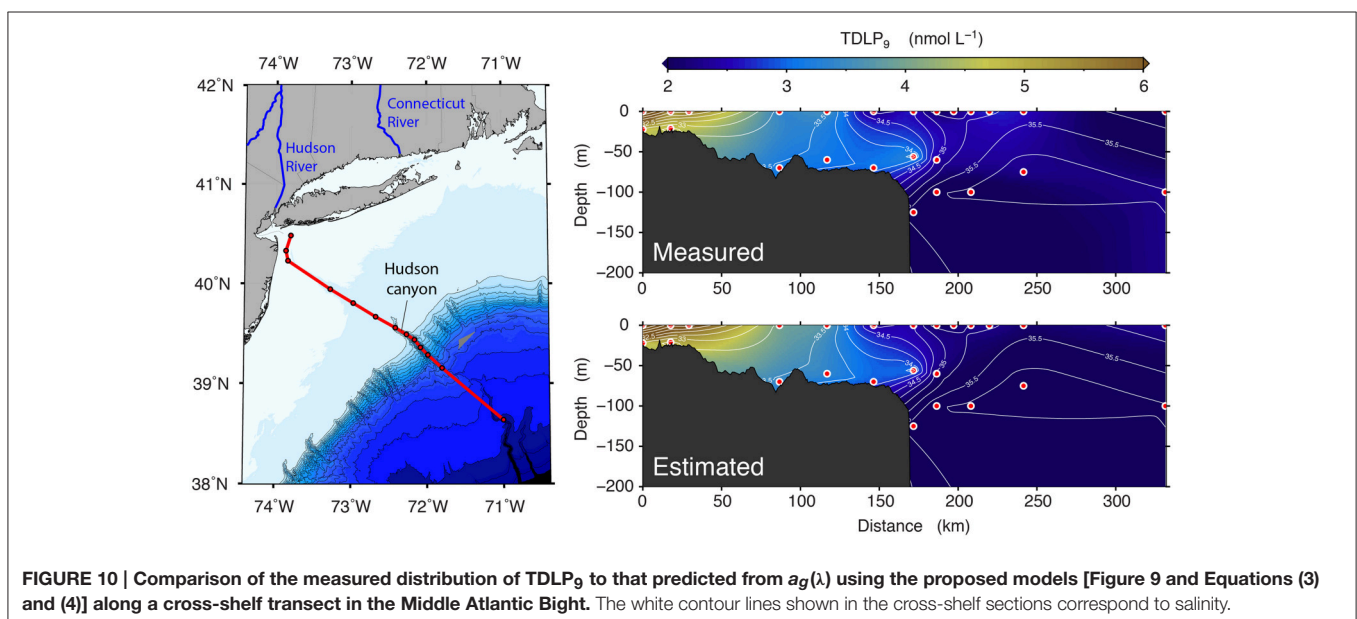


**FIGURE 10 | Comparison of the measured distribution of TDLP<sub>9</sub> to that predicted from  $a_g(\lambda)$  using the proposed models [Figure 9 and Equations (3) and (4)] along a cross-shelf transect in the Middle Atlantic Bight. The white contour lines shown in the cross-shelf sections correspond to salinity.**

model adequately reproduced the most important features of the measured-TDLP<sub>9</sub> distribution along the salinity gradient. For instance, the cross-shelf gradient from the lignin-rich mouth of the Hudson River to the depleted open waters of the Middle Atlantic Bight was well-reproduced, just like the subsurface TDLP<sub>9</sub> maximum measured at the entrance of Hudson canyon. The more subtle features of the TDLP<sub>9</sub> distribution were less well-reproduced. The average error of  $\pm 20\%$  associated with the retrievals implies that the model can only reproduce significant gradients in lignin.

The model is expected to perform similarly well in most river-influenced coastal oceans of the world, as long as the TDLP<sub>9</sub> predictions are made within the ranges of  $a_g(\lambda)$  and TDLP<sub>9</sub>-values used to train the model. The variety of coastal environments represented in this data set suggests the model will be suitable for most sub-tropical, temperate, and Arctic coastal oceans that receive notable inputs of terrigenous DOM. However, the performance of the model remains uncertain in coastal regions influenced by tropical rivers, as these were not represented in the training data set. More importantly, the use of the model is not recommended in major coastal upwelling systems that typically receive little terrigenous DOM inputs (e.g., California current, Benguela current). In these coastal water types, autochthonous sources of DOM are likely to exert a more dominant control on the dynamics of  $a_g(\lambda)$ , and the link between TDLP<sub>9</sub> and  $a_g(\lambda)$  is likely to deviate significantly from the relationship established. Naturally, this simple model is not final, and can be very easily re-trained to improve and expand its applicability as more data become available.

## AUTHOR CONTRIBUTIONS

CF, RB, KK, CL, and HO collected the *in situ* samples for CDOM and lignin analysis. CF, KK, YS, and CL processed the lignin samples, and CF, YS, CL, and RA processed the CDOM samples. CF wrote the manuscript with important discussion with RB, KK, YS, and RA and with comments from all authors.

## REFERENCES

- Aiken, G. R., and Cotsaris, E. (1995). Soil and Hydrology: their effects on NOM. *J. Am. Water Work. Assoc.* 87, 36–45.
- Aiken, G. R., McKnight, D. M., Wershaw, R. L., and MacCarthy, P. (eds.). (1985). “Humic substances,” in *Soil, Sediment, and Water: Geochemistry, Isolation and Characterization* (New York, NY: John Wiley & Sons), 363–385.
- Alberts, J. J. (1982). The effect of metal ions on the ultraviolet spectra of humic acid, tannic acid and lignosulfonic acid. *Water Res.* 16, 1273–1276. doi: 10.1016/0043-1354(82)90146-4
- Amon, R. M. W., Rinehart, A. J., Duan, S., Louchouart, P., Prokushkin, A., Guggenberger, G., et al. (2012). Dissolved organic matter sources in large Arctic rivers. *Geochim. Cosmochim. Acta* 94, 217–237. doi: 10.1016/j.gca.2012.07.015
- Benner, R., Hatcher, P. G., and Hedges, J. I. (1990). Early diagenesis of mangrove leaves in a tropical estuary: bulk chemical characterization using solid-state <sup>13</sup>C NMR and elemental analyses. *Geochim. Cosmochim. Acta* 54, 2003–2013. doi: 10.1016/0016-7037(90)90268-P

## ACKNOWLEDGMENTS

Most of the data used in this study were collected during research cruises carried out as part of the following projects: (1) the Malina Scientific Program (<http://malina.obs-vlfr.fr>) funded by ANR (Agence nationale de la recherche), INSU-CNRS (Institut national des sciences de l'univers, Centre national de la recherche scientifique), CNES (Centre national d'études spatiales), and ESA (European Space Agency); (2) the Circumpolar Flaw Lead (CFL) study ([http://www.ipy-api.gc.ca/pg\\_IPYAPI\\_029-eng.html](http://www.ipy-api.gc.ca/pg_IPYAPI_029-eng.html)) funded by the Government of Canada (IPY #96); (3) the Impacts of Climate on the Eco-Systems and Chemistry of the Arctic Pacific Environment (ICESCAPE) program (<http://www.espo.nasa.gov/icescape/>) funded by NASA (National Aeronautics and Space Administration); (4) the Nansen and Amundsen Basin Observational System (NABOS) project (<http://nabos.iarc.uaf.edu/index.php>) funded by the US-NSF (National Science Foundation), NOAA (National Oceanographic and Atmospheric Administration), the ONR (Office of Naval Research), and JAMSTEC (Japan Marine Science and Technology Center), (5) the GulfCarbon project funded by the National Science Foundation ([http://ocean.otr.usm.edu/~w301130/research/gulfcarbon\\_new.htm](http://ocean.otr.usm.edu/~w301130/research/gulfcarbon_new.htm)), and (6) the University-National Oceanographic Laboratory System (UNOLS) 2013 chief scientist training cruise sponsored by the National Science Foundation (<https://www.unols.org/chief-scientist-training-cruise>) and supported under NSF grant OCE-1230900. The Otsuchi Bay samples were collected as part of the research program “Tohoku Ecosystem-Associated Marine Sciences” (TEAMS) of the Ministry of Education, Culture, Sports, Science and Technology (MEXT). This work was directly supported by NSF grants 0713915 and 0850653 to R.B., and NSF grants 0229302, 0425582, 0713991 to R.M.W.A. We thank the following people: the crews of the R/V Cape Hatteras, R/V Hugh Sharp, R/V Endeavor, USCGC Healy, CCGS Amundsen, and Russian icebreaker *Kapitan Dranitsyn* for assistance with sample collection, Dr. Jolynn Carroll for collecting the Gulf-of-Ob samples, Stephanie Smith and Sally Walker for absorbance measurements on the NABOS samples, and Steven E. Lohrenz and Wei-Jun Cai for providing berths on the GulfCarbon cruises.

- Benner, R., and Kaiser, K. (2011). Biological and photochemical transformations of amino acids and lignin phenols in riverine dissolved organic matter. *Biogeochemistry* 102, 209–222. doi: 10.1007/s10533-010-9435-4
- Benner, R., and Opsahl, S. (2001). Molecular indicators of the sources and transformations of dissolved organic matter in the Mississippi river plume. *Org. Geochem.* 32, 597–611. doi: 10.1016/S0146-6380(00)00197-2
- Benner, R., Peele, E. R., and Hodson, R. E. (1986). Microbial utilization of dissolved organic matter from leaves of the red mangrove, *Rhizophora mangle*, in the Fresh Creek estuary, Bahamas. *Estuar. Coast. Shelf Sci.* 23, 607–619. doi: 10.1016/0272-7714(86)90102-2
- Boyle, E. S., Guerriero, N., Thiallet, A., Del Vecchio, R., and Blough, N. V. (2009). Optical properties of humic substances and CDOM: relation to structure. *Environ. Sci. Technol.* 43, 2262–2268. doi: 10.1021/es803264g
- Chapman, D. C., and Beardsley, R. C. (1989). On the origin of shelf water in the Middle Atlantic Bight. *J. Phys. Oceanogr.* 19, 384–391.

- Chin, Y., Aiken, G., and O'Loughlin, E. (1994). Molecular weight, polydispersity, and spectroscopic properties of aquatic humic substances. *Environ. Sci. Technol.* 28, 1853–1858.
- Cota, G. F., Pomeroy, L. R., Harrison, W. G., Jones, E. P., Peters, F., Sheldon, W. M., et al. (1996). Nutrients, primary production and microbial heterotrophy in the southeastern Chukchi Sea: Arctic summer nutrient depletion and heterotrophy. *Mar. Ecol. Prog. Ser.* 135, 247–258. doi: 10.3354/meps135247
- Del Vecchio, R., and Blough, N. V. (2004). On the origin of the optical properties of humic substances. *Environ. Sci. Technol.* 38, 3885–3891. doi: 10.1021/es049912h
- Dittmar, T., de Rezende, C. E., Manecki, M., Niggemann, J., Coelho Ovalle, A. R., Stubbins, A., et al. (2012). Continuous flux of dissolved black carbon from a vanished tropical forest biome. *Nat. Geosci.* 5, 618–622. doi: 10.1038/ngeo1541
- Dittmar, T., and Kattner, G. (2003). The biogeochemistry of the river and shelf ecosystem of the Arctic Ocean: a review. *Mar. Chem.* 83, 103–120. doi: 10.1016/S0304-4203(03)00105-1
- Eriksson, K.-E. (2010). "Lignin Biodegradation," in *Lignin and Lignans*, eds C. Heitner, D. R. Dimmel, and J. A. Schmidt (Boca Raton, FL: CRC Press), 495–520.
- Fichot, C. G., and Benner, R. (2011). A novel method to estimate DOC concentrations from CDOM absorption coefficients in coastal waters. *Geophys. Res. Lett.* 38:L03610. doi: 10.1029/2010gl046152
- Fichot, C. G., and Benner, R. (2012). The spectral slope coefficient of chromophoric dissolved organic matter (S275–S295) as a tracer of terrigenous dissolved organic carbon in river-influenced ocean margins. *Limnol. Oceanogr.* 57, 1453–1466. doi: 10.4319/lo.2012.57.5.1453
- Fichot, C. G., and Benner, R. (2014). The fate of terrigenous dissolved organic carbon in a river-influenced ocean margin. *Global Biogeochem. Cycles* 28, 300–318. doi: 10.1002/2013GB004670
- Fichot, C. G., Kaiser, K., Hooker, S. B., Amon, R. M. W., Babin, M., Bélanger, S., et al. (2013). Pan-Arctic distributions of continental runoff in the Arctic Ocean. *Sci. Rep.* 3, 1053. doi: 10.1038/srep01053
- Fichot, C. G., Lohrenz, S. E., and Benner, R. (2014). Pulsed, cross-shelf export of terrigenous dissolved organic carbon to the Gulf of Mexico. *J. Geophys. Res. Ocean.* 119, 1176–1194. doi: 10.1002/2013JC009424
- Fukuda, H., Ogawa, H., Sohrin, R., Yamasaki, A., and Koike, I. (2007). Sources of dissolved organic carbon and nitrogen in Otsuchi Bay on the Sanriku ria coast of Japan in the spring. *Coast. Mar. Sci.* 31, 19–29.
- Furman, G. S., and Lonsky, W. F. W. (1988a). Charge-transfer complexes in kraft lignin part 1: occurrence. *J. Wood Chem. Technol.* 8, 165–189.
- Furman, G. S., and Lonsky, W. F. W. (1988b). Charge-transfer complexes in kraft lignin part 2: contribution to color. *J. Wood Chem. Technol.* 8, 191–208.
- Goni, M. A., Monacci, N., Gisewhite, R., Crockett, J., Nitttrouer, C., Ogston, A., et al. (2008). Terrigenous organic matter in sediments from the Fly River delta-clinofan system (Papua New Guinea). *J. Geophys. Res. Earth Surf.* 113. doi: 10.1029/2006jf000653
- Grebmeier, J. M. (2012). Shifting patterns of life in the Pacific Arctic and Sub-Arctic Seas. *Ann. Rev. Mar. Sci.* 4, 63–78. doi: 10.1146/annurev-marine-120710-100926
- Hedges, J. I., and Ertel, J. R. (1982). Characterization of lignin by gas capillary chromatography of cupric oxide oxidation products. *Anal. Chem.* 54, 174–178. doi: 10.1021/ac00239a007
- Hedges, J. I., Keil, R. G., and Benner, R. (1997). What happens to terrestrial organic matter in the ocean? *Org. Geochem.* 27, 195–212. doi: 10.1016/S0146-6380(97)00066-1
- Hedges, J. I., and Mann, D. C. (1979). The characterization of plant tissues by their lignin oxidation products. *Geochim. Cosmochim. Acta* 43, 1803–1807. doi: 10.1016/0016-7037(79)90028-0
- Helms, J. R., Stubbins, A., Perdue, E. M., Green, N. W., Chen, H., and Mopper, K. (2013). Photochemical bleaching of oceanic dissolved organic matter and its effect on absorption spectral slope and fluorescence. *Mar. Chem.* 155, 81–91. doi: 10.1016/j.marchem.2013.05.015
- Helms, J. R., Stubbins, A., Ritchie, J. D., Minor, E. C., Kieber, D. J., and Mopper, K. (2008). Absorption spectral slopes and slope ratios as indicators of molecular weight, source, and photobleaching of chromophoric dissolved organic matter. *Limnol. Oceanogr.* 53, 955–969. doi: 10.4319/lo.2008.53.3.0955
- Hernes, P. J., and Benner, R. (2003). Photochemical and microbial degradation of dissolved lignin phenols: Implications for the fate of terrigenous dissolved organic matter in marine environments. *J. Geophys. Res.* 108. doi: 10.1029/2002jc001421
- Hernes, P. J., and Benner, R. (2006). Terrigenous organic matter sources and reactivity in the North Atlantic Ocean and a comparison to the Arctic and Pacific oceans. *Mar. Chem.* 100, 66–79. doi: 10.1016/j.marchem.2005.11.003
- Hernes, P. J., Benner, R., Cowie, G. L., Goni, M. A., Bergamaschi, B. A., and Hedges, J. I. (2001). Tannin diagenesis in mangrove leaves from a tropical estuary: a novel molecular approach. *Geochim. Cosmochim. Acta* 65, 3109–3122. doi: 10.1016/S0016-7037(01)00641-X
- Hernes, P. J., Bergamaschi, B. A., Eckard, R. S., and Spencer, R. G. M. (2009). Fluorescence-based proxies for lignin in freshwater dissolved organic matter. *J. Geophys. Res. Biogeosci.* 114, 1–10. doi: 10.1029/2009JG000938
- Jaffé, R., Ding, Y., Niggemann, J., Vähätalo, A. V., Stubbins, A., Spencer, R. G. M., et al. (2013). Global charcoal mobilization from soils via dissolution and riverine transport to the oceans. *Science* 340, 345–347. doi: 10.1126/science.1231476
- Kaiser, K., and Benner, R. (2012). Characterization of lignin by gas chromatography and mass spectrometry using a simplified CuO oxidation method. *Anal. Chem.* 84, 459–464. doi: 10.1021/ac202004r
- Kieber, D. J., McDaniel, J., and Mopper, K. (1989). Photochemical source of biological substrates in sea water: implications for carbon cycling. *Nature* 341, 637–639. doi: 10.1038/341637a0
- Kieber, R. J., Zhou, X., and Mopper, K. (1990). Formation of carbonyl compounds from UV-induced photodegradation of humic substances in natural waters: fate of riverine carbon in the sea. *Limnol. Oceanogr.* 35, 1503–1515. doi: 10.4319/lo.1990.35.7.1503
- Kim, S., Kaplan, L. A., Benner, R., and Hatcher, P. G. (2004). Hydrogen-deficient molecules in natural riverine water samples - Evidence for the existence of black carbon in DOM. *Mar. Chem.* 92, 225–234. doi: 10.1016/j.marchem.2004.06.042
- Kraus, T. E., Dahlgren, R. A., and Zasoski, R. J. (2003). Tannins in nutrient dynamics of forest ecosystems - a review. *Plant Soil* 256, 41–66. doi: 10.1023/A:1026206511084
- Lawrence, J. (1980). Semi-quantitative determination of fulvic acid, tannin and lignin in natural waters. *Water Res.* 14, 373–377. doi: 10.1016/0043-1354(80)90085-8
- Louchouart, P., Opsahl, S., and Benner, R. (2000). Isolation and quantification of dissolved lignin from natural waters using solid-phase extraction and GC/MS. *Anal. Chem.* 72, 2780–2787. doi: 10.1021/ac9912552
- Maie, N., Jaffé, R., Miyoshi, T., and Childers, D. L. (2006). Quantitative and qualitative aspects of dissolved organic carbon leached from senescent plants in an oligotrophic wetland. *Biogeochemistry* 78, 285–314. doi: 10.1007/s10533-005-4329-6
- Maie, N., Pisani, O., and Jaffé, R. (2008). Mangrove tannins in aquatic ecosystems: their fate and possible influence on dissolved organic carbon and nitrogen cycling. *Limnol. Oceanogr.* 53, 160–171. doi: 10.4319/lo.2008.53.1.0160
- Mannino, A., and Harvey, H. R. (2004). Black carbon in estuarine and coastal ocean dissolved organic matter. *Limnol. Oceanogr.* 49, 735–740. doi: 10.4319/lo.2004.49.3.0735
- Martone, P. T., Estevez, J. M., Lu, F., Ruel, K., Denny, M. W., Somerville, C., et al. (2009). Discovery of lignin in seaweed reveals convergent evolution of cell-wall architecture. *Curr. Biol.* 19, 169–175. doi: 10.1016/j.cub.2008.12.031
- Medeiros, P. M., Seidel, M., Ward, N. D., Carpenter, E. J., Gomes, H. R., Niggemann, J., et al. (2015). Fate of the Amazon River dissolved organic matter in the tropical Atlantic Ocean. *Global Biogeochem. Cycles* 29:2015GB005115. doi: 10.1002/2015GB005115
- Miller, W. L., Moran, M. A., Sheldon, W. M., Zepp, R. G., and Opsahl, S. (2002). Determination of apparent quantum yield spectra for the formation of biologically labile photoproducts. *Limnol. Oceanogr.* 47, 343–352. doi: 10.4319/lo.2002.47.2.0343
- Mountain, D. G. (1991). The volume of Shelf Water in the Middle Atlantic Bight: seasonal and interannual variability, 1977–1987. *Cont. Shelf Res.* 11, 251–267. doi: 10.1016/0278-4343(91)90068-H
- Nelson, N. B., Carlson, C. A., and Steinberg, D. K. (2004). Production of chromophoric dissolved organic matter by Sargasso Sea microbes. *Mar. Chem.* 89, 273–287. doi: 10.1016/j.marchem.2004.02.017
- Opsahl, S., and Benner, R. (1995). Early diagenesis of vascular plant tissues: lignin and cutin decomposition and biogeochemical implications. *Geochim. Cosmochim. Acta* 59, 4889–4904. doi: 10.1016/0016-7037(95)00348-7

- Opsahl, S., and Benner, R. (1997). Distribution and cycling of terrigenous dissolved organic matter in the ocean. *Nature* 386, 480–482. doi: 10.1038/386480a0
- Opsahl, S., and Benner, R. (1998). Photochemical reactivity of dissolved lignin in river and ocean waters. *Limnol. Oceanogr.* 43, 1297–1304. doi: 10.4319/lo.1998.43.6.1297
- Opsahl, S., Benner, R., and Amon, R. M. W. (1999). Major flux of terrigenous dissolved organic matter through the Arctic Ocean. *Limnol. Oceanogr.* 44, 2017–2023. doi: 10.4319/lo.1999.44.8.2017
- Ortega-Retuerta, E., Frazer, T. K., Duarte, C. M., Ruiz-Halpern, S., Tovar-Sánchez, A., Arrieta, J., et al. (2009). Biodegradation of chromophoric dissolved organic matter by bacteria and krill in the Southern Ocean. *Limnol. Oceanogr.* 54, 1941–1950. doi: 10.4319/lo.2009.54.6.1941
- Osburn, C. L., and Stedmon, C. A. (2011). Linking the chemical and optical properties of dissolved organic matter in the Baltic-North Sea transition zone to differentiate three allochthonous inputs. *Mar. Chem.* 126, 281–294. doi: 10.1016/j.marchem.2011.06.007
- Palmer, M. A., van Dijken, G. L., Greg Mitchell, B., Seegers, B. J., Lowry, K. E., Mills, M. M., et al. (2013). Light and nutrient control of photosynthesis in natural phytoplankton populations from the Chukchi and Beaufort seas, Arctic Ocean. *Limnol. Oceanogr.* 58, 2185–2205. doi: 10.4319/lo.2013.58.6.2185
- Philben, M., Kaiser, K., and Benner, R. (2014). Biochemical evidence for minimal vegetation change in peatlands of the West Siberian lowland during the medieval climate anomaly and little ice age. *J. Geophys. Res. Biogeosci.* 119, 808–825. doi: 10.1002/2013JG002396
- Rochelle-Newall, E. J., and Fisher, T. R. (2002). Production of chromophoric dissolved organic matter fluorescence in marine and estuarine environments: an investigation into the role of phytoplankton. *Mar. Chem.* 77, 7–21. doi: 10.1016/S0304-4203(01)00072-X
- Russo, C., Stanzione, F., Alfè, M., Ciajolo, A., and Tregrossi, A. (2012). Spectral analysis in the UV-visible range for revealing the molecular form of combustion-generated carbonaceous species. *Combust. Sci. Technol.* 184, 1219–1231. doi: 10.1080/00102202.2012.664315
- Schiller, R. V., Kourafalou, V. H., Hogan, P., and Walker, N. D. (2011). The dynamics of the Mississippi River plume: impact of topography, wind and offshore forcing on the fate of plume waters. *J. Geophys. Res. Ocean.* 116. doi: 10.1029/2010jc006883
- Schmidt, J. (2010). “Electronic Spectroscopy of Lignins,” in *Lignin and Lignans*, eds C. Heitner, D. R. Dimmel, and J. A. Schmidt (Boca Raton, FL: CRC Press), 49–102.
- Sharpless, C. M., and Blough, N. V. (2014). The importance of charge-transfer interactions in determining chromophoric dissolved organic matter (CDOM) optical and photochemical properties. *Environ. Sci. Process. Impacts* 16, 654–671. doi: 10.1039/c3em00573a
- Shen, Y., Fichot, C. G., and Benner, R. (2012a). Dissolved organic matter composition and bioavailability reflect ecosystem productivity in the Western Arctic Ocean. *Biogeosciences* 9, 4993–5005. doi: 10.5194/bg-9-4993-2012
- Shen, Y., Fichot, C. G., and Benner, R. (2012b). Floodplain influence on dissolved organic matter composition and export from the Mississippi-Atchafalaya River system to the Gulf of Mexico. *Limnol. Oceanogr.* 57, 1149–1160. doi: 10.4319/lo.2012.57.4.1149
- Spencer, R. G. M., Aiken, G. R., Wickland, K. P., Striegl, R. G., and Hernes, P. J. (2008). Seasonal and spatial variability in dissolved organic matter quantity and composition from the Yukon River basin, Alaska. *Global Biogeochem. Cycles* 22, 1–13. doi: 10.1029/2008GB003231
- Spencer, R. G. M., Stubbins, A., Hernes, P. J., Baker, A., Mopper, K., Aufdenkampe, A. K., et al. (2009). Photochemical degradation of dissolved organic matter and dissolved lignin phenols from the Congo River. *J. Geophys. Res. Biogeosci.* 114, 1–12. doi: 10.1029/2009JG000968
- Stubbins, A., Spencer, R. G. M., Mann, P. J., Holmes, R. M., McClelland, J. W., Niggemann, J., et al. (2015). Utilizing colored dissolved organic matter to derive dissolved black carbon export by arctic rivers. *Front. Earth Sci.* 3:63. doi: 10.3389/feart.2015.00063
- Tesi, T., Semiletov, I., Hugelius, G., Dudarev, O., Kuhry, P., and Gustafsson, Ö. (2014). Composition and fate of terrigenous organic matter along the Arctic land-ocean continuum in East Siberia: insights from biomarkers and carbon isotopes. *Geochim. Cosmochim. Acta* 133, 235–256. doi: 10.1016/j.gca.2014.02.045
- Tzortziou, M., Neale, P. J., Osburn, C. L., Megonigal, J. P., Maie, N., and Jaffé, R. (2008). Tidal marshes as a source of optically and chemically distinctive colored dissolved organic matter in the Chesapeake Bay. *Limnol. Oceanogr.* 53, 148–159. doi: 10.4319/lo.2008.53.1.0148
- Walker, S. A., Amon, R. M. W., Stedmon, C., Duan, S., and Louchouart, P. (2009). The use of PARAFAC modeling to trace terrestrial dissolved organic matter and fingerprint water masses in coastal Canadian Arctic surface waters. *J. Geophys. Res. Biogeosci.* 114, 1–12. doi: 10.1029/2009JG000990
- Weishaar, J., and Aiken, G. (2001). Evaluation of specific ultra-violet absorbance as an indicator of the chemical content of dissolved organic carbon. *Environ. Chem.* 41, 843–845. doi: 10.1021/es030360x
- Yamashita, Y., Fichot, C. G., Shen, Y., Jaffé, R., and Benner, R. (2015). Linkages among fluorescent dissolved organic matter, dissolved amino acids and lignin-derived phenols in a river-influenced ocean margin. *Front. Mar. Sci.* 2:92. doi: 10.3389/fmars.2015.00092
- Yamashita, Y., Nosaka, Y., Suzuki, K., Ogawa, H., Takahashi, K., and Saito, H. (2013). Photobleaching as a factor controlling spectral characteristics of chromophoric dissolved organic matter in open ocean. *Biogeosciences* 10, 7207–7217. doi: 10.5194/bg-10-7207-2013
- Yamashita, Y., and Tanoue, E. (2008). Production of bio-refractory fluorescent dissolved organic matter in the ocean interior. *Nat. Geosci.* 1, 579–582. doi: 10.1038/ngeo279
- Zhang, Y., van Dijk, M. A., Liu, M., Zhu, G., and Qin, B. (2009). The contribution of phytoplankton degradation to chromophoric dissolved organic matter (CDOM) in eutrophic shallow lakes: field and experimental evidence. *Water Res.* 43, 4685–4697. doi: 10.1016/j.watres.2009.07.024
- Ziolkowski, L. A., and Druffel, E. R. M. (2010). Aged black carbon identified in marine dissolved organic carbon. *Geophys. Res. Lett.* 37, 4–7. doi: 10.1029/2010GL043963

**Conflict of Interest Statement:** The authors declare that the research was conducted in the absence of any commercial or financial relationships that could be construed as a potential conflict of interest.

Copyright © 2016 Fichot, Benner, Kaiser, Shen, Amon, Ogawa and Lu. This is an open-access article distributed under the terms of the Creative Commons Attribution License (CC BY). The use, distribution or reproduction in other forums is permitted, provided the original author(s) or licensor are credited and that the original publication in this journal is cited, in accordance with accepted academic practice. No use, distribution or reproduction is permitted which does not comply with these terms.